HHS Public Access

Author manuscript

Proc SPIE Int Soc Opt Eng. Author manuscript; available in PMC 2011 September 18.

Published in final edited form as:

Proc SPIE Int Soc Opt Eng. 2010 March 5; 7546(1): . doi:10.1117/12.861259.

Near-IR Imaging of Thermal Changes in Enamel during Laser Ablation

Linn H. Maung, **Chulsung Lee**, and **Daniel Fried***

Department of Preventive and Restorative Dental Sciences, University of California, San Francisco, School of Dentistry, CA 94143-0758

Abstract

The objective of this work was to observe the various thermal-induced optical changes that occur in the near-infrared (NIR) during drilling in dentin and enamel with the laser and the high-speed dental handpiece. Tooth sections of ~ 3 mm-thickness were prepared from extracted human incisors (N=60). Samples were ablated with a mechanically scanned CO_2 laser operating at a wavelength of 9.3-μm, a 300-Hz laser pulse repetition rate, and a laser pulse duration of 10–20 μs. An InGaAs imaging camera was used to acquire real-time NIR images at 1300-nm of thermal and mechanical changes (cracks). Enamel was rapidly removed by the CO_2 laser without peripheral thermal damage by mechanically scanning the laser beam while a water spray was used to cool the sample. Comparison of the peripheral thermal and mechanical changes produced while cutting with the laser and the high-speed hand-piece suggest that enamel and dentin can be removed at high speed by the CO_2 laser without excessive peripheral thermal or mechanical damage. Only 2 of the 15 samples ablated with the laser showed the formation of small cracks while 9 out of 15 samples exhibited crack formation with the dental hand-piece. The first indication of thermal change is a decrease in transparency due to loss of the mobile water from pores in the enamel which increase light-scattering. To test the hypothesis that peripheral thermal changes were caused by loss of mobile water in the enamel, thermal changes were intentionally induced by heating the surface. The mean attenuation coefficient of enamel increased significantly from 2.12 ± 0.82 to 5.08 ± 0.98 with loss of mobile water due to heating.

Keywords

near-infrared imaging; CO_2 laser; dental hard tissues; laser ablation; thermal damage

2. INTRODUCTION

Over the past two years we have presented work showing that near-IR (NIR) imaging can be used to image the formation of craters during IR laser ablation since the enamel of the tooth is almost completely transparent near 1310-nm (1–3). These studies showed that there is great potential for NIR imaging to monitor laser-ablation events in real-time to assess safe laser operating parameters by imaging thermal and stress-induced damage, elaborate the

*Contact Author: daniel.fried@ucsf.edu.

mechanisms involved in ablation such as dehydration, monitor removal of demineralized enamel and investigate the dynamic changes in the transparency of enamel with water loss. Other NIR imaging studies have demonstrated that NIR light at 1310-nm is ideally suited for the transillumination of interproximal dental caries (dental decay in between teeth) and that it can also be used to image decay in the pits and fissures of the occlusal (biting) surfaces of posterior teeth where most new dental decay occurs and even image interproximal lesions from the occlusal surface(4–7). In this paper, we present further NIR imaging measurements involving laser ablation with a mechanically scanned 9.3-μm CO_2 laser system in which the laser beam is scanned over a two dimensional pattern on the enamel surface for efficient and rapid removal of enamel without peripheral thermal damage. In a previous study, we found that excessive heat accumulation near the laser incisions caused loss of transparency in the enamel and dynamic changes in that transparency were directly visible during laser irradiation. One objective of this work was to carry out additional measurements to elucidate the mechanism of those changes and confirm the hypothesis that those changes are due to the loss of mobile water in the enamel. The loss of mobile water located in the interprismatic spaces of the enamel is likely to leave pores that act as scattering sites in the enamel reducing it's transparency. Enamel contains about 10% water by volume, half of that water is located in between the enamel prisms while the other half is bound as waters of hydration in the enamel mineral phase. The magnitude of the optical changes were determined by measuring the attenuation of NIR light before and after laser irradiation and after heating the enamel with other thermal sources. Optical tomographic imaging studies show reduced optical penetration if the extracted teeth being imaged are allowed to desiccate (dry out), therefore these measurements are also important for determining the optimum conditions for imaging dental caries in the NIR (5, 8, 9).

Since NIR imaging works so well for viewing peripheral and thermal damage in real-time around incisions made by lasers. We postulated that it would work equally well for drilling with the high-speed hand-piece. Moreover, since small cracks are sometimes created peripheral to the laser incisions even under conditions that are ideal to minimize thermal damage, we also desired to determine if such crack formation was unique to those laser conditions and determine if similar cracks are formed with a similar frequency while cutting with the high-speed dental hand-piece. Therefore, the peripheral thermal and mechanical damage after drilling with the laser and the high-speed dental hand-piece was compared.

3. MATERIALS AND METHODS

3.1 Tooth Samples

Sixty tooth sections approximately 3-mm thick were prepared from extracted human 3rd molars and incisors that were stored in water with only 0.1% thymol added to inhibit bacteria and fungal growth. Surfaces were serially polished to a finish of 0.1-μm using embedded diamond polishing discs. Sections were chosen that had the best enamel "windows" for viewing.

3.2 Near Infrared Imaging (near-IR)

A three component, modular 7X NIR precision zoom lens consisting of a focusable lower module, a manual upper zoom module and a 1.5 TV tube from Edmund Scientific (Barrington, NJ) was used with the InGaAs focal plane array (FPA). The field of view was adjustable from 0.81 to 5.6-mm, the magnification from 1.7X to 11.8X, and the numerical aperture from 0.036 to 0.12. Light from a 150-W fiber-optic illuminator FOI-1 E Licht Company (Denver, CO) coupled to an adjustable aperture and a 90-nm bandpass filter centered at 1310-nm, Filter# BP-1300-090-B Spectrogon US Inc. (Parsippany, NJ) was used to illuminate the samples. A high sensitivity InGaAs FPA, Model SU320KTSX from Sensors Unlimited (Princeton, NJ) with 320 × 240 pixels (25-μm) was used to acquire all the images. The 8-bit digital video was acquired using a digital video recorder.

3.3 Ablation Apparatus

Samples were irradiated using an industrial marking laser, Impact 2500 from GSI Lumonics (Rugby, United Kingdom) operating at a wavelength of 9.3 μm. The laser was custom modified to produce a Gaussian output beam (single spatial mode) and a pulse duration of between 10–15-μs. This laser is capable of high repetition rates up to 500 Hz, and a fixed repetition rate of 300 Hz was used for all of these experiments. The laser energy output was monitored using a power meter EPM 1000, Coherent-Molectron (Santa Clara, CA), and the Joulemeter ED-200 from Gentec (Quebec, Canada). The laser beam was focused to a spot size of ~300-μm using a planoconvex ZnSe lens of 125-mm focal length. A razor blade was scanned across the beam to determine the diameter ($1/e^2$) of the laser beam. The laser energy was up to 25 mJ per pulse for incedent fluence of up to 40 J/cm^2. Two and three dimensional images of the laser spatial profile was acquired using a Pyrocam™ I pyroelectric array from Spirocon (Logan, UT). Both laser beam profile and spatial profile showed that the laser was operated in a single spatial mode, i.e., Gaussian spatial beam. Holes were produced in samples at either a fixed position or by scanning the laser-beam at a rate of 1.5-mm/sec by fixing the laser-hand-piece to a computer-controlled linear stage. Repetition rate of 20 to 300- Hz were used for the experiments. Sub-ablative measurements were performed by defocusing the laser beam incident on the tooth surface. Computer-controlled XY galvanometers 6200HM series with MicroMax Series 671 from Cambridge Technology, Inc. (Cambridge) were used to scan the laser beam over sample surfaces. A low volume/low pressure air- actuated fluid spray delivery system consisting of a 780S spray valve, a Valvemate 7040 controller, and a fluid reservoir from EFD, Inc. (East Providence, RI) was used to provide a uniform spray of fine water mist onto the tooth surfaces at 2 mL/min.

3.4 Experimental Procedures

In the initial series of experiments, cylindrical incisions were cut using the CO_2 laser at a fluence of 40 J/cm^2 and a repetition rate of 300 Hz with a water spray. The laser beam was scanned across the tooth section at a rate of 1.5 mm/sec. In the next series of experiments designed to deliberately produce thermal damage, the CO_2 laser was defocused so that non-ablative irradiation intensities were incident on the tooth surface ablation causing only localized heating on seven tooth sections that were irradiated with a repetition rate of 100

Hz. A small heat gun Model P-1K from Portasol (Carlow, Ireland) was also used to locally heat the tooth sections to cause reversible changes in transparency.

In the last series of experiments we compared the peripheral thermal and mechanical damage produced by a standard dental hand-piece with the laser. Holes were drilled using a high-speed air turbine with a fresh #330 diamond bur.

4. RESULTS

For the first group of samples, rectangular incisions 1 mm × 0.5 mm were produced in 15 samples as shown in Fig. 2 by mechanically scanning the CO_2 laser beam in 2 dimensions using galvanometer scanners with a repetition rate of 300 Hz on the tooth sample, while a low volume water spray was applied to the surface of the sample. The laser beam diameter was 300 microns, and rectangular craters are formed on the samples by scanning rapidly from the apex to the root direction. Each laser spot or position was separated by 100 microns to provide a high degree of overlap to form a smooth and even ablation crater. The InGaAs FPA was used to capture 8-bit video at the rate of ten frames a second during the ablation process, so that the evolution of the ablation crater along with enamel opacity changes (increase in the attenuation coefficient) and mechanical damages (crack formation) on the sample could be recorded in real time.

The crater shown in Fig. 2 was formed by ablation at a repetition rate of 300 Hz and 100 passes for total of 1000 laser pulses. The craters extend into the enamel by more than 2-mm, and there were no changes in the appearance of the peripheral enamel suggesting that there is minimal peripheral thermal damage. During the ablation process, concentric radial patterns of varying intensity emanate from the site of ablation and propagate in the direction of the dentinal-enamel junction (DEJ). It is not clear that these radial structures represent shock waves, stress waves or thermal gradients in the samples. Out of 15 samples that were ablated employing the same parameters, only 2 were found to have produced small cracks peripheral to the ablation crater. Figure 3 shows the formation of a small crack on one the samples, which terminates at the DEJ. The other crack exhibited similar behavior, namely starting at the end of ablation crater and ending at the DEJ. If water-cooling is not used during ablation, peripheral mechanical and thermal damage is observed even at lower scanning rates. The surrounding sound enamel was observed to have increased opacity and cracks were formed that often propagated well into the dentin.

The peripheral thermal and mechanical damage caused by the high-speed dental hand-piece was also investigated for comparison with the laser preparations. Holes were drilled using a high-speed dental hand piece with a fresh #330 diamond bur. The evolution of the preparation was also monitored in real-time. One fundamental difference between drilling with the laser versus the hand-piece is that efficient drilling with the hand-piece requires considerable skill and is operator and technique sensitive. The condition of the bur also can profoundly influence peripheral thermal and mechanical damage. Therefore, the enamel was removed conservatively with a generous volume of the water spray applied during the drilling. Nevertheless, 9 out of 15 samples that were prepared using the high-speed hand-piece exhibited mechanical damage (cracks) and some of the samples showed changes in the

opacity of the peripheral enamel indicative of thermal damage. Figure 4 shows a tooth section during drilling with the bur. A couple of small cracks were formed at the base of the preparation.

Some of the optical changes that occurred in the enamel were reversible with rehydration which suggests that these changes in the transparent enamel are mostly caused by the loss of mobile water phase from enamel pores [2]. Additional measurements were carried out to shed further light on the mechanism of these changes and quantify those changes. Samples were irradiated by a defocused laser beam at a repetition rate of 100-Hz in order to rapidly deposit heat on the surface of the enamel. As the enamel is heated without ablation the opacity increases and the enamel becomes opaque to a similar level as the more highly scattering enamel. All the samples manifested an initial delay of several seconds before the onset loss of optical changes. This delay can easily be explained as the time required reach a sufficient temperature rise to produce the thermally induced changes. For most of the samples an advancing front behind which the enamel has reduced transparency propagates from the enamel surface where the heat deposition is taking place into the interior of the tooth towards the DEJ. However, in some of the samples there was the highly unusual observation that the advancing front began at the DEJ and approached the enamel surface. Figure 5 shows a sample irradiated by the defocused laser beam with the front advancing from the DEJ towards the surface of the tooth and the position of that front is indicated by the red arrows. The change in opacity may be dependent on the internal pore structure, the local water content and prism orientation in addition to the temperature rise, which may provide an explanation for the lower threshold at the DEJ on some of the samples.

Some of the samples were heated by a miniature butane heat gun with a ¼ inch nozzle. This enabled localized heating of the sample surface. The heat gun produced similar changes in the enamel transparency to that observed during laser heating which confirms this effect is caused by heat accumulation. Fig. 6 shows a sample before heating, after heating and after rehydration. The sample lost transparency after heating and then subsequently regained transparency after immersion in water for several hours. The changes in attenuation coefficient of the enamel were calculated by using for six of the samples. The mean attenuation coefficient of enamel increased significantly from 2.12 ± 0.82 to 5.076 ± 0.98 ($p<0.05$) with the loss of mobile water phase from the enamel pores ($n=6$).

5. DISCUSSION

Laser ablation craters could be imaged through sound human tooth sections of approximately 3-mm thickness with high detail during their formation. Clean ablation craters were produced rapidly with minimal loss of efficiency with increasing depth. One problem with dental hard tissue ablation at CO_2 laser wavelengths is that highly conical ablation craters are produced for fixed spot ablation or if the laser is scanned in only one direction. Although this can be explained as a purely geometrical effect leading to decreasing fluence as the conical crater develops over repeated laser pulses, it appears worse for the 9.3 and 9.6-μm wavelengths that manifest high reflectance. The imaginary component of the refractive index at those wavelengths gives rise to reflectance values approaching 50% (10, 11).

It appears that ablation can be more efficient if small spot sizes are employed and the laser is scanned in two dimensions during ablation. In the companion paper in this proceeding (Nguyen et al.), we demonstrate that scanning the laser in two dimensions avoids stalling and excessive heat accumulation allowing the rapid removal of enamel at 300-Hz without producing an excessive temperature rise in the pulp. In a previous study using a similar spot size, we found that if the laser was scanned along only one axis the ablation rapidly stalled and the heat accumulation subsequently exceeded safe levels (12). Although the highly conical ablation holes may seem to be a significant disadvantage, it adds an additional level of safety, since upon failure of the scanner, the laser is unlikely to drill a deep hole through the dentin and into the pulp. Excessive heat accumulation will still occur but that takes a considerable amount of time and the clinician and patient are likely to have sufficient time to recognize the problem. Peripheral thermal and mechanical damage were minimized as well and only two small cracks were observed for 15 samples. A comparison with the high-speed drill indicated that there were less cracks produced with the laser 2/15 vs. 9/15 for the drill. Moreover, some of the samples prepared with the drill showed some peripheral thermal changes indicative of peripheral thermal damage.

Additional studies were carried out regarding the reversible, thermally induced optical changes observed in enamel. Attenuation measurements indicated that light scattering in the enamel increased by 2–3 cm^{-1} at 1310-nm after the thermal changes. This change is sufficient to produce the dramatic change observed in the highly transparent enamel in the near-IR since the attenuation is at least a factor of two higher than the sound enamel. However, such a change in the visible range where the sound enamel has a scattering coefficient near 60 cm^{-1} (13) would be hardly noticeable which may explain why such a phenomenon has not be reported previously.

Stress waves or thermal gradients originating from the site of ablation were observed propagating through the samples during drilling and the nature and origin of those waves warrant further investigation. Moreover, initial thermal changes were noted close to the DEJ in some of the samples as opposed to the position closest to the site of irradiation and future studies will investigate this phenomenon as well.

ACKNOWLEDGEMENTS

This study was supported by NIDCR grants R01-DE19631 + T32 DE0073060. The authors would also like to acknowledge the contributions of Cynthia L. Darling.

REFERENCES

1. Darling C, Fried D. Real-time near-IR imaging of ablation crater formation in dental enamel during laser ablation. Lasers in Dentistry XIII. 2007; Vol. 6425:I1–I6.
2. Darling C, Fried D. Real-time near-IR imaging of ablation crater formation in dental enamel during laser ablation. Optics Express. 2008; 16(4):2685–2693. [PubMed: 18542353]
3. Darling CL, Maffei ME, Fried WA, Fried D. Near-IR imaging of erbium laser ablation with a water spray. Lasers in Dentistry XIV. 2008; Vol. 6843:1–7.
4. Bühler CM, Ngaotheppitak P, Fried D. Imaging of occlusal dental caries (decay) with near-IR light at 1310-nm. Optics Express. 2005; 13(2):573–582. [PubMed: 19488387]

5. Jones RS, Huynh GD, Jones GC, Fried D. Near-IR Transillumination at 1310-nm for the Imaging of Early Dental Caries. Optics Express. 2003; 11(18):2259–2265. [PubMed: 19466117]
6. Fried, D.; Featherstone, JDB.; Darling, CL.; Jones, RS.; Ngaotheppitak, P.; Buehler, CM. Early Caries Imaging and Monitoring with Near-IR Light, Dental clinics of North America. Philadelphia: W. B Saunders Company; 2005.
7. Fried D, Buhler CM, Ngaotheppitak P, Darling CL. Near-IR imaging of interproximal lesions from occlusal surfaces and the influence of stains and plaque. 2006; Vol. 6137:1–7.
8. Fried D, Xie J, Shafi S, Featherstone JDB, Breunig T, Lee CQ. Early detection of dental caries and lesion progression with polarization sensitive optical coherence tomography. J. Biomed. Optics. 2002; 7(4):618–627.
9. Jones RS, Fried D. The Effect of High Index Liquids on PS-OCT Imaging of Dental Caries. Lasers in Dentistry XI. 2005; Vol. 5687:34–41.
10. Duplain G, Boulay R, Belanger PA. Complex index of refraction of dental enamel at CO_2 wavelengths. Appl. Optics. 1987; 26:4447–4451.
11. Fried D, Glena RE, Featherstone JDB, Seka W. Permanent and transient changes in the reflectance of CO_2 laser irradiated dental hard tissues at λ=9.3, 9.6, 10.3, and 10.6 μm and at fluences of 1–20 J/cm^2. Lasers in Surg. Med. 1997; 20:22–31. [PubMed: 9041504]
12. Pierre, D. MS Thesis. San Francisco: University of California, San Francisco; 2007. Pulpal Safety Study Using A Long Pulse 9.3-μm TEA CO_2 Laser Operating At High Repetition Rates.
13. Fried D, Featherstone JDB, Glena RE, Seka W. The nature of light scattering in dental enamel and dentin at visible and near-IR wavelengths. Appl. Optics. 1995; 34(7):1278–1285.

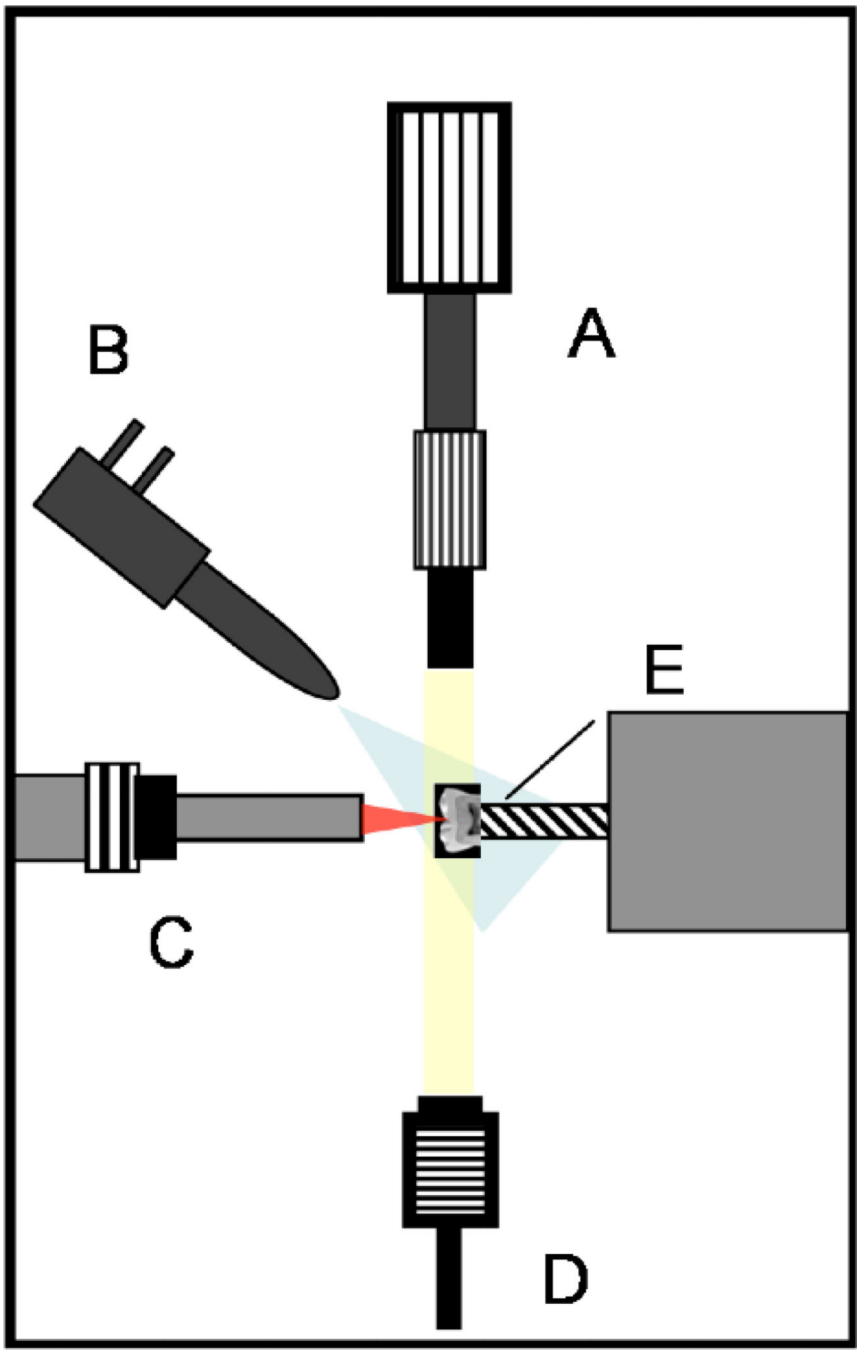

Fig. 1.
Imaging Setup. (A) InGaAs FPA with zoom lens, (B) water spray nozzle, (C) laser hand-piece, (D) fiber-optic illuminator, (E) sample holder and tooth section.

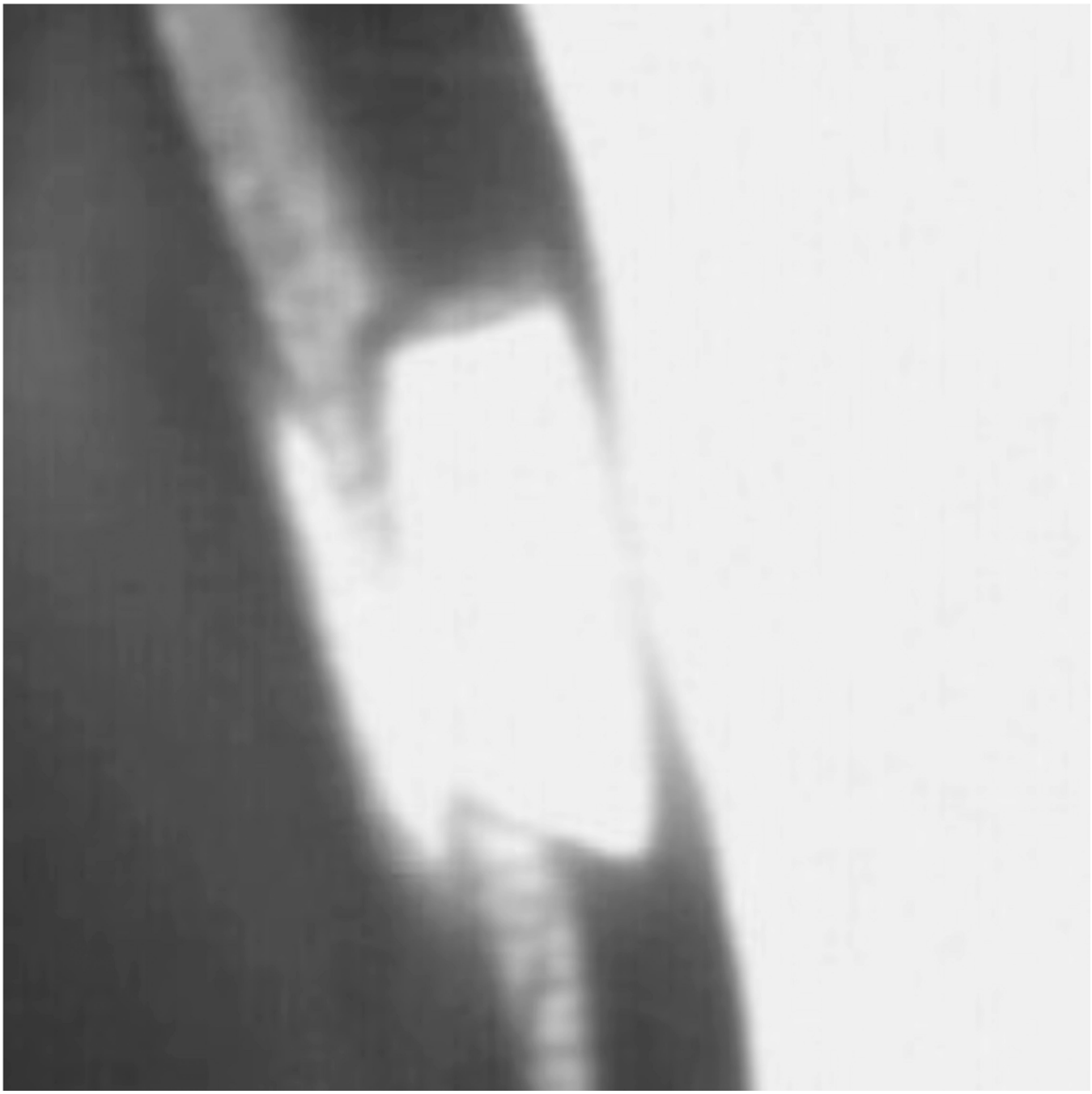

Fig. 2.
Image of tooth section during scanning ablation at 300-Hz. Minimal peripheral thermal damage is visible.

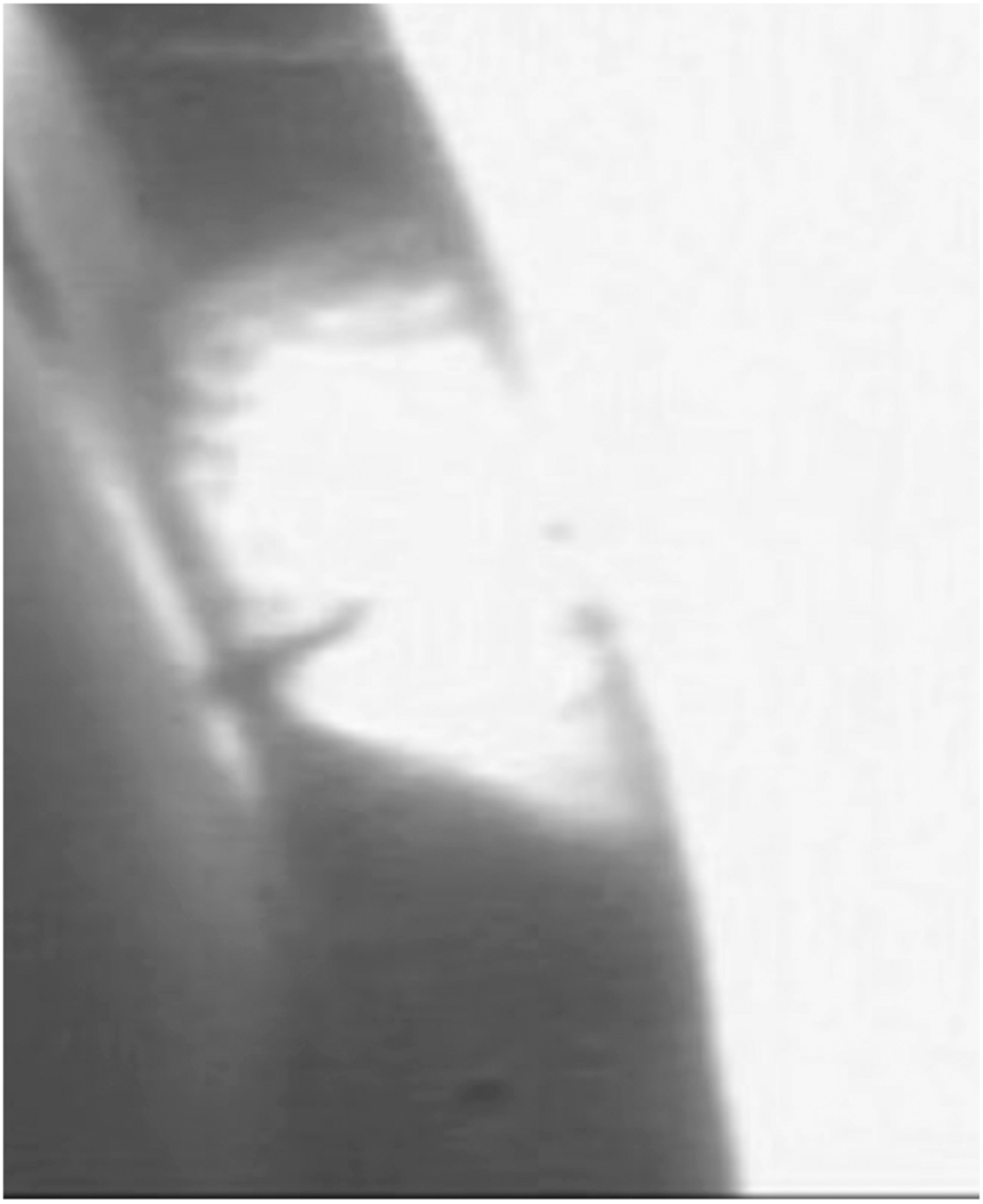

Fig. 3.

Image of tooth section during scanning ablation at 300-Hz. The formation of a small crack is visible during ablation. ***See attached multimedia file (video1)***. http://dx.doi.org/10.1117/12.849333.1.

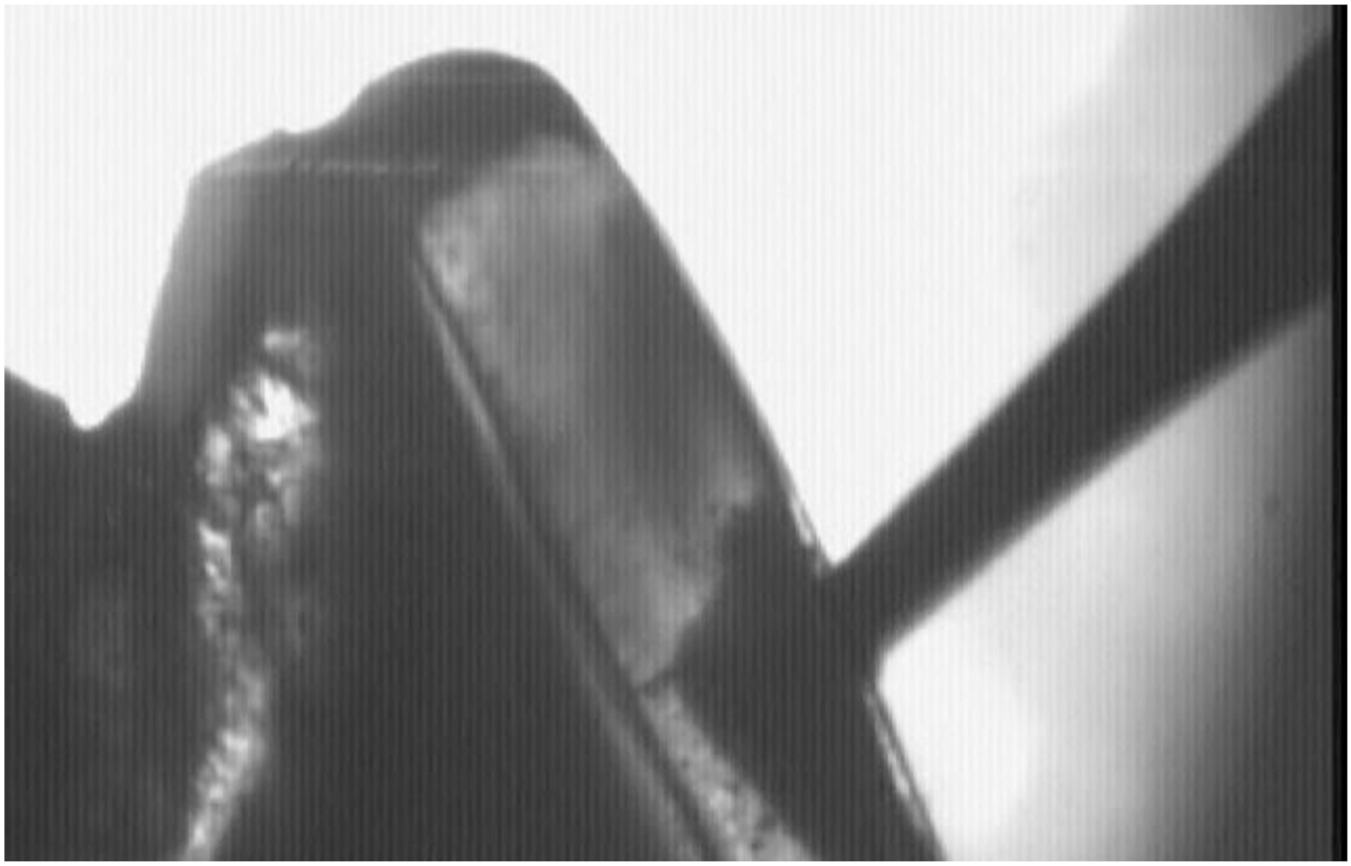

Fig. 4.

Image of tooth section during cutting with a dental bur. The formation of a small crack is visible during ablation. ***See attached multimedia file (video2)***. http://dx.doi.org/10.1117/12.849333.2.

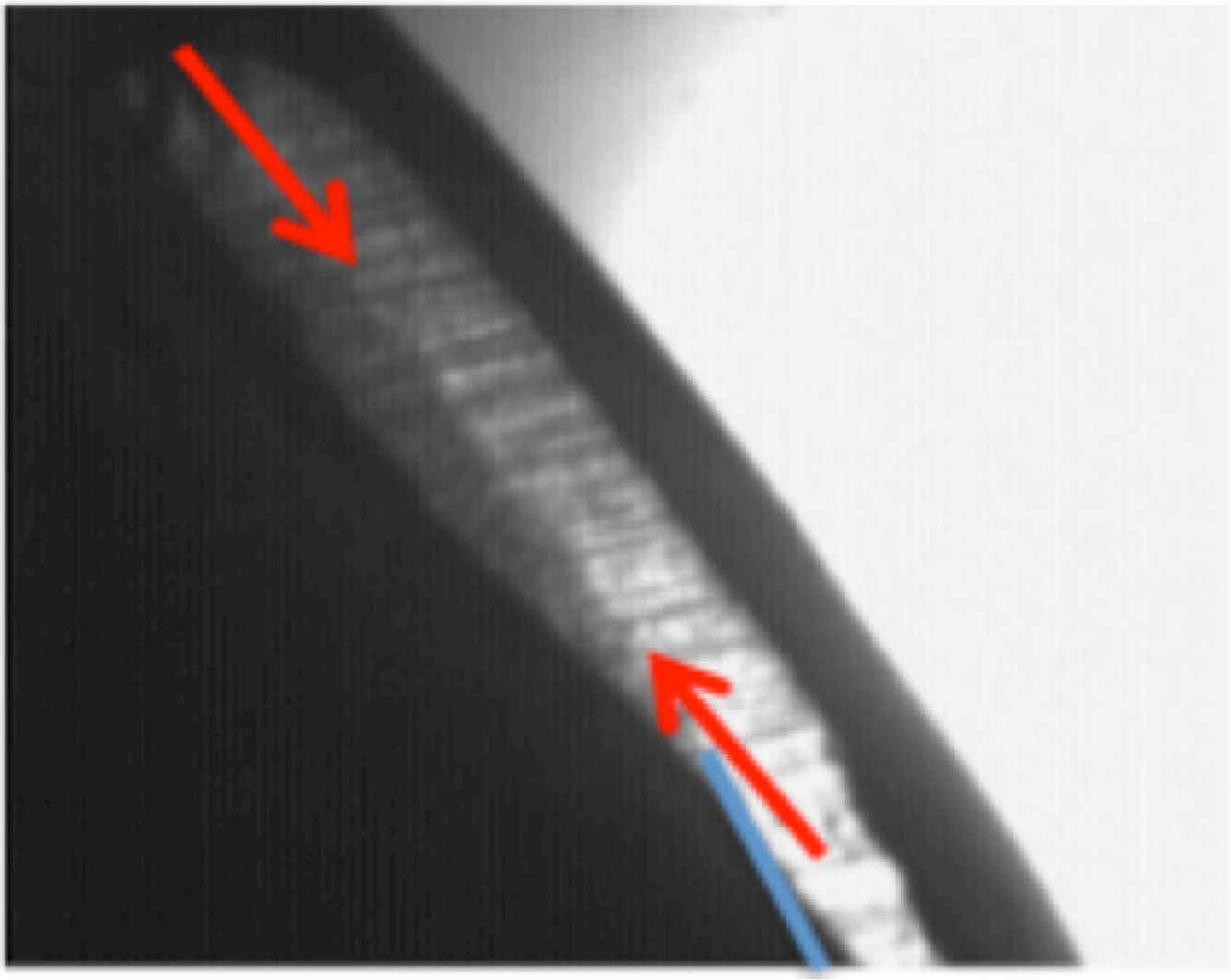

Fig. 5.

Image of tooth section showing optic changes due to desiccation actually propagating outward from the dentinal-enamel junction during laser irradiation at non-ablative irradiation intensities.

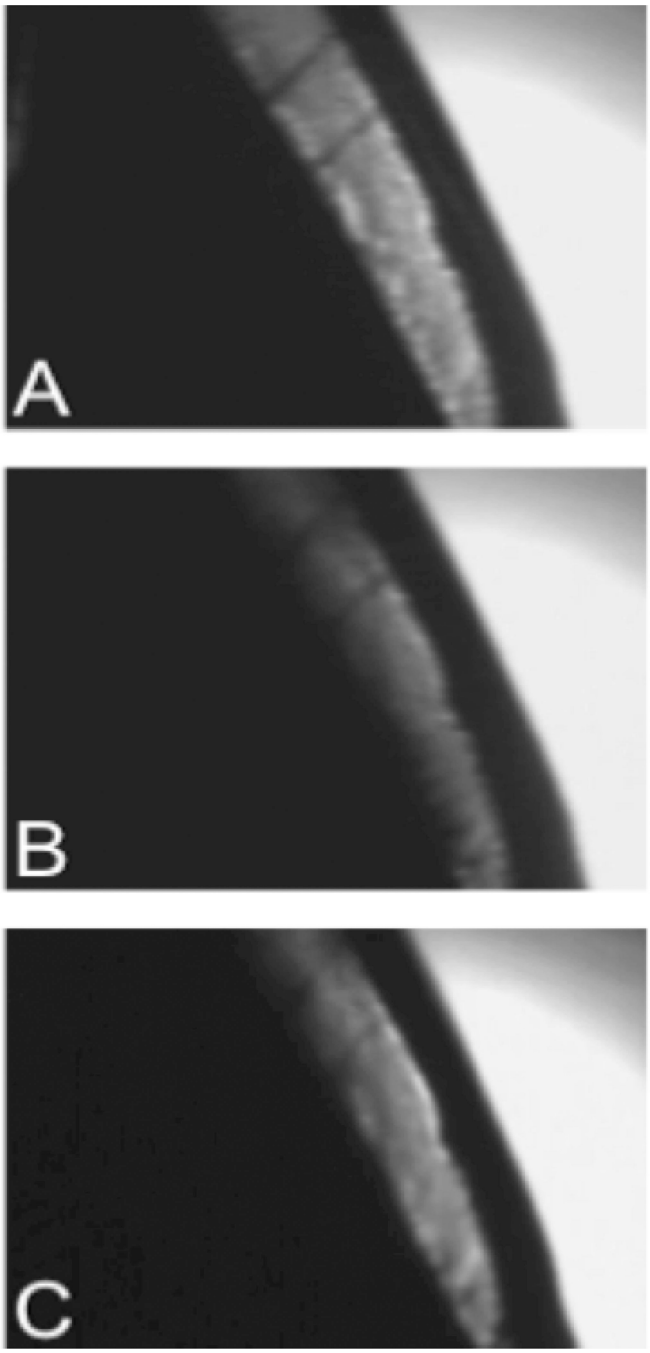

Fig. 6.

Image of tooth section showing optic changes due to desiccation by external heating using a miniature butane heat gun, (A) before, (B) after heating and (C) after rehydration. ***See attached multimedia file (video3)***. http://dx.doi.org/1 0.1117/12.849333.3